Batteries & Supercaps

Research Article
doi.org/10.1002/batt.202200001

Chemistry Europe
European Chemical Societies Publishing

www.batteries-supercaps.org

Special Collection

Low Current-Density Stable Zinc-Metal Batteries Via Aqueous/Organic Hybrid Electrolyte

Yue Chen,[a] Shan Guo,[a] Liping Qin,*[b] Qiangwei Wan,[a] Yicai Pan,[a] Miao Zhou,[a] Mengqiu Long,[d] Guozhao Fang,*[a] and Shuquan Liang*[a, c]

Zinc-metal batteries (ZMBs) are promising for large-scale energy storage devices due to their intrinsically safe, low-cost and environmentally friendly nature. ZMBs with vanadium-based cathodes have exhibited excellent performance, however, many side reactions due to the presence of innumerable water molecules in aqueous electrolyte hinder their commercialization. Herein, high-proportioned polyethylene glycol was introduced as solvent to form an aqueous/organic hybrid electrolyte, which limits the activity of free water molecules and lowers the risk of side reactions, such as cathode dissolution, zinc dendrites and H_2 evolution. As a result, a good reversible zinc plating/stripping over 3000 h for zinc anode and an excellent cycle stability with 96% retention after 50 cycles at low current density of 0.1 $A g^{-1}$ for vanadium-based cathode were obtained, respectively. Importantly, to simulate the stability in actual application environment, a test mode at low current density under both continuous and intermittent electrochemical charge/discharge was conducted, which further demonstrated the superiority of this hybrid electrolyte. Finally, as a practical illustration, the pouch cells of 3 cm × 3 cm exhibit a high capacity of 300 $mAh g^{-1}$ at 0.1 $A g^{-1}$ with a good retention of 81.7% after 200 cycles, and even up to 500 cycles at 0.5 $A g^{-1}$. This work is expected to provide new opportunities for high-performance hybrid electrolyte for the practical ZMBs.

Introduction

Aqueous zinc-metal batteries (ZMBs) are the most promising energy storage system for large-scale energy storage system due to their merits with intrinsic safety and low cost.[1–4] Compared with other cathode materials,[5] vanadium (V)-based compounds with rich variety and high theoretical capacity have been widely developed to serve as cathodes of ZMBs.[6,7] Although several outstanding performances of V-based cathodes, such as the long-term stability at ultrahigh rates[8,9] and good suitability at low-temperature environment,[10] have been ascertained by many reports, it suffers severe capacity attenuation under low current densities (e.g., below 0.5 $A g^{-1}$), which is a key metric for the practical application of ZMBs. The long-term reliability in realistic conditions is more crucial, which needs to work at a low current density. Moreover, to date, the cycling stability of ZMBs is mainly evaluated based on the continuous electrochemical condition, which is quite different from the actual application environment with the characteristics of intermittent use. A more reliable test mode containing the cycling capacity and the anti-self-discharge behavior is needed to estimate the performance of V-based cathode accurately, albeit at the lab-scale. However, this critical problem has received little attention and limited solution strategy.

The capacity attenuation at low current densities caused by the cathode side could be ascribed to: (1) A deeper Zn^{2+} ion intercalation/extraction at low current densities, which is more likely to cause serious deformation of the host material structure; (2) cathode dissolution results in a loss of active substances, leading to the self-discharge behavior and an unstable electrode/electrolyte interface. The structural engineering strategy by introducing pillars, such as H_2O,[9,11] Na^+,[12] Zn^{2+}[13] and Ca^{2+}[14] into the interlayers of V_2O_5 could mitigate the structural strain caused by the repeated insertion/extraction of Zn^{2+}. However, the self-discharge effect of ZMBs as capacity fading at low current densities is still severe, which is the bottleneck problem restricting the commercial application. On the other hand, many undesired issues on the anode side still exist due to the presence of a large amount of active water in aqueous electrolyte, such as water splitting, Zn dendrite and byproducts formation.[15–17] Therefore, an effective and feasible strategy to improve the cycling performance of ZMBs based on V_2O_5 cathode at low current densities with practical consideration is urgently needed to be developed.

[a] Y. Chen, S. Guo, Q. Wan, Y. Pan, M. Zhou, Prof. G. Fang, Prof. S. Liang
School of Materials Science and Engineering
Central South University
Changsha 410083, Hunan, China
E-mail: fg_zhao@csu.edu.cn
lsq@csu.edu.cn
[b] Prof. L. Qin
College of Biological and Chemical Engineering
Guangxi University of Science and Technology
Liuzhou 545006, Guangxi, China
E-mail: qinlp2005@126.com
[c] Prof. S. Liang
Key Laboratory of Electronic Packaging and Advanced Functional Materials of Hunan Province
Central South University
Changsha 410083, Hunan, China
[d] Prof. M. Long
School of Physics and Electronics
Central South University
Changsha 410083, Hunan, China

Supporting information for this article is available on the WWW under https://doi.org/10.1002/batt.202200001

Special Collection An invited contribution to a Special Collection dedicated to Aqueous Electrolyte Batteries

Research Article
doi.org/10.1002/batt.202200001
Chemistry Europe
European Chemical Societies Publishing

As a part of battery, electrolyte has a great impact on the overall performance of the battery.[18,19] Many endeavors have been made to pursue a more suitable combination of electrodes and electrolytes.[20,21] Exploration of new aqueous electrolyte chemistries to achieve a robust interface becomes important unprecedentedly.[22] Electrolyte modulation by using high concentrated electrolyte is considered as a facile approach to stabilize the interface. Zhang and co-workers[23] employed "water-in-salt" electrolyte (WiSE) to $Zn/Ca_{0.2}V_2O_5 \cdot 0.8H_2O$ battery. Impressively, the capacity retention increases from 8.4% to 51.1% over 100 cycles at a low current rate of 50 mA g^{-1} with the increasing concentration of aqueous $ZnCl_2$ electrolytes from 1 m (mol kg^{-1}, molality) to 30 m. Previous research has established that WiSE, with features of a larger electrochemical stability window (ESW, ~3.0 V) and alleviated water-induced side reactions, renders an unprecedented opportunity to overcome the water-induced dreadful side reactions.[24] However, the high-cost trait of WiSE sets up a formidable challenge to provide wide applications for stationary grid storage.[25] Another promising way to suppress the water activity is introducing additives with affordable prices, such as CH_3OH,[26] CH_3CH_2OH,[27] CH_3CN (AN),[28] dimethyl sulfoxide[29,30] and so on. In particular, Zhang et al.[31] reported a non-concentrated aqueous electrolyte composed of 2 m $Zn(CF_3SO_3)_2$ and organic dimethyl carbonate (DMC) additives to stabilize the Zn electrochemistry. Additionally, the dissolution of V_2O_5 electrode materials was suppressed when organic solvents were added. It is a truism that organic solvents are usually toxic and have a pungent smell, which deviates from the original intention of intrinsically safe. Therefore, strategies to develop eco-friendly and low-cost aqueous electrolytes with a wide voltage window to achieve safe, high-energy ZMBs are necessary.

Polyethylene glycol 400 (PEG 400, $HO(CH_2CH_2O)_nH$, $M_n = 400$) with a wide range of compatibility with various solutions, is a common humectant used in liquid preparations, such as oral liquid. It was reckoned that PEG 400 as additives could reduce the water activity,[32] alleviating the issues of water-induced side reactions. In addition, PEG 400 is cheaper than other organic solvents, such as AN and DMC, which is an appropriate choice for preparing non-toxic and low-cost electrolytes. Herein, we construct a practical, eco-friendly and low-cost electrolyte by introducing PEG 400 as a co-solvent into non-concentrated (1 m) aqueous electrolyte. From the results of linear sweep voltammetry, molecular dynamics (MD) simulations, Fourier transform infrared spectroscopy (FTIR) and proton nuclear magnetic resonance (^{1}H NMR), it was found that the hydroxyl group in PEG could effectively suppress the water activity by hydrogen bonding. Our electrolyte exhibits a wide ESW of 2.6 V, reducing the risk of gas evolution of hydrogen (or oxygen) on the surface of the electrodes and the dissolution of $V_2O_5 \cdot nH_2O$ (HVO) cathode. Consequently, the hybrid aqueous coin-cells and pouch-cells based on HVO cathode achieves remarkable cycling stability at a low current density of 0.1 A g^{-1}, and even under an intermittent electrochemical test.

Results and Discussion

Structure and characterization of designed hybrid electrolyte

To investigate the efficacy of PEG 400 component, we constructed a series of $Zn(CF_3SO_3)_2$ (ZOT)-based electrolytes containing PEG 400 with a weight ratio from 50% to 60%, 70%, 80% and 90%. ZSO is not a good solute in the hybrid solvent as the ratio of PEG increases, as shown in Figure S1. The ignition tests intuitively identified the nonflammable nature of the aqueous/PEG 400 hybrid electrolytes (Figure S2). Although the existence of viscous PEG reduces the ionic conductivity of aqueous electrolyte, electrolyte with such a high content of above 50% PEG still remains a high ionic conductivity of 7.8 mS cm^{-1} (Figure S3).

The interaction between solute and solvent of prepared electrolytes above were investigated including ^{1}H NMR and FTIR. The ^{1}H NMR spectra demonstrates that the ^{1}H chemical shift in H_2O (3.96 ppm) experiences a downshift (high filed) with increasing PEG content (Figure 1a). This evolution indicates an increase of electron density around the H atom upon the addition of PEG, which can be attributed to the hydrogen-bonding interaction between the O atom of PEG and the H atom in H_2O.[33] When the electrolyte contains 60% PEG, the ^{1}H chemical shift in H_2O becomes very weak, meaning the great enhancement of hydrogen-bonding interaction. As the further increase of PEG, ^{1}H chemical of H in methylene in PEG overlaps that of the water molecule.[34] The H-bond formation in hybrid electrolytes was confirmed by FTIR spectra (Figure S4). The blue shift (lower wave-number) of O–H stretching and O–H bending vibrations indicates that the O–H covalent bond strength is increased, which is ascribed to the decrease of large complexes of water molecules interconnected by hydrogen bonding as the content of PEG increases.[35] The PEG addition partially restricts the water mobility imposed by hydrogen bonding between water clusters and the ethereal oxygen atom in PEG. These results demonstrated the suppression of water activity by addition of PEG.

To decipher the role of PEG in electrolyte and the coordination structure of Zn^{2+}, molecular dynamics (MD) simulations were performed for 1 m ZOT-H_2O and 1 m ZOT-H_2O-*x*%PEG (Figure S5). Zn^{2+} is typically coordinated with 6 H_2O molecules in 1 m ZOT-H_2O-0% PEG to form $Zn(H_2O)_6^{2+}$ solvate. Corresponding the radial distribution functions (RDFs), the coordination number of water molecules in the primary solvation sheath decreases to 2 in 1 m ZOT-H_2O-90% PEG (Figure S6f). With the increase of PEG content, the coordination water in the first solvation layer gradually decreased (Figure 1b), and the anion salt gradually increased (Figure 1c). When the PEG content above 60%, the coordination number of H_2O decrease below 4. The increasing trend of coordination number of PEG in the primary sheath is similar to the downward trend of that of coordinated water (Figure S7). While the primarily coordination number of OTf^- anions augments to ~1.5, and then followed a little increase as the PEG content increases from 60% to 90%. Besides, it can be seen that there a huge increase of coordinated O (PEG) but a negligible increase

Research Article
doi.org/10.1002/batt.202200001
Chemistry Europe
European Chemical Societies Publishing

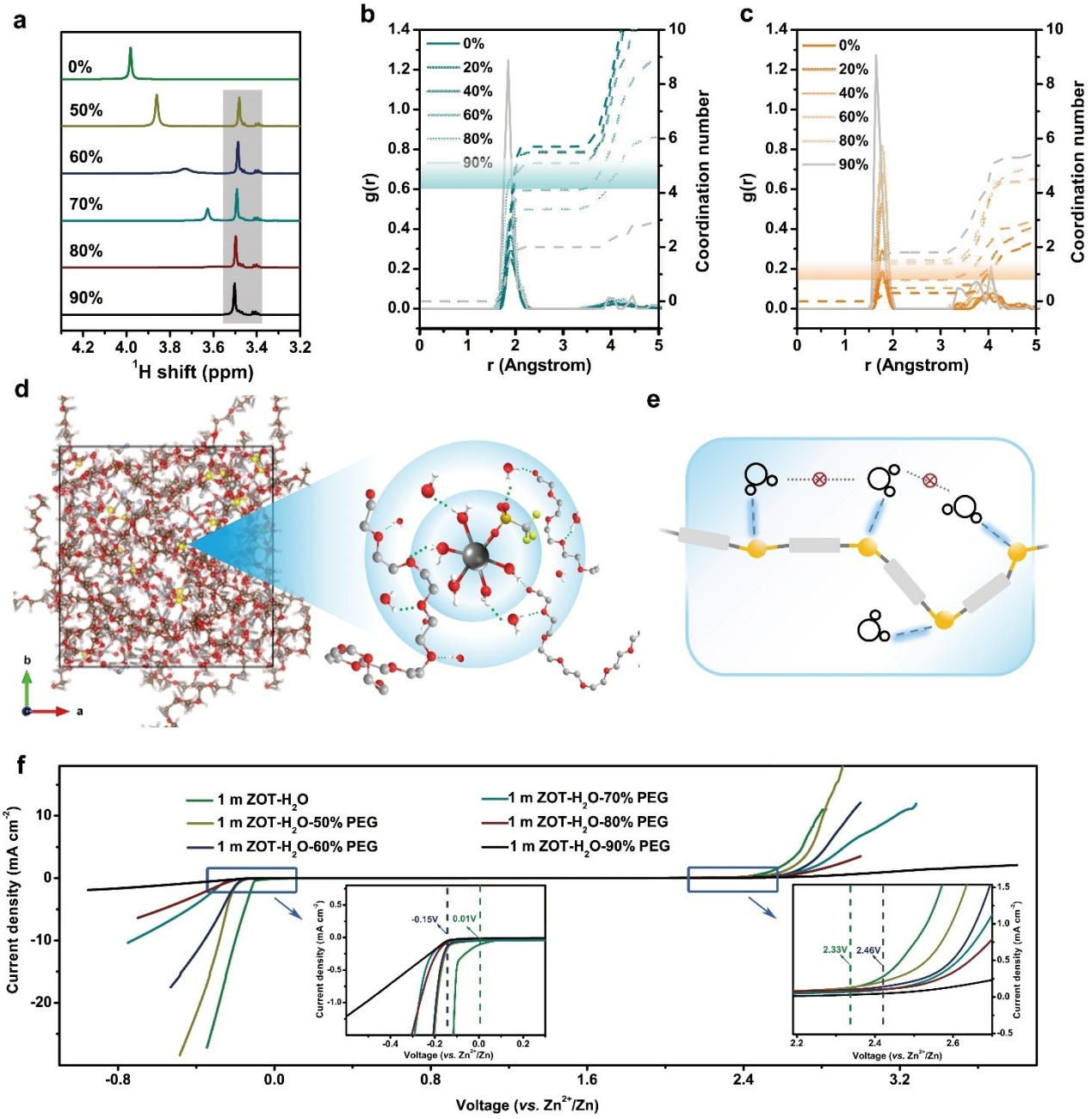

Figure 1. a) ^{1}H NMR spectra of 1 m ZOT-H_2O-*x*% PEG electrolyte. RDFs (solid line) and the coordination number (dotted line) in 1 m ZOT-H_2O-*x*% PEG electrolyte of: b) Zn–O(H_2O), c) Zn–O(OTf^-). d) Snapshots of the MD simulations and the representing solvation structures for 1 m ZOT-H_2O-60% PEG. e) Schematic illustration of the bonds between H_2O molecular and PEG. f) The ESW of electrolytes determined by LSV. Insets are the magnified views of the regions marked near anodic (HER) and cathodic (OER) extremes.

of coordinated O (anion) when the PEG content increase to above 60%. Therefore, 60% PEG is inferred to be an appropriate content to modulate the hybrid electrolyte. The optimized electrolyte formula (1 m ZOT-H_2O-60% PEG electrolyte) was chosen for further research on its electrochemical performance, as discussed later.

In 1 m ZOT-H_2O-60% PEG electrolyte (Figure 1d), the OTf^- anion occur in the Zn^{2+}-solvation structure, and the coordinated H_2O in the solvation sheath is further confined by the hydroxyl group in the long-chain PEG. Besides, the amount of free water molecules is greatly decreased by the addition of high-content PEG. This is suggested that there is a higher proportion of coordinated water than free water, which will greatly reduce the water splitting (Figure 1e).

The linear sweep voltammetry (LSV) experiments also confirm that the overall ESW of electrolytes significantly improves as the PEG content increases, compared to that of 1 m ZOT-H_2O electrolyte (Figure 1f).[26] For 1 m ZOT-H_2O-60% PEG, the hydrogen evolution reaction (HER) potential decreases from 0.01 V (vs. Zn^{2+}/Zn) to −0.15 V, and the potential of

Research Article
doi.org/10.1002/batt.202200001
Chemistry Europe
European Chemical Societies Publishing

oxygen evolution reaction (OER) shifts from 2.33 V to 2.46 V, resulting in a wide ESW of 2.6 V. Such shifts of HER and OER could attributed to the reduction of free water molecules in the hybrid electrolyte.[24]

Compatibility between hybrid electrolyte and Zn anode

Zn/Zn symmetric cells were used to illustrate compatibility and stability of hybrid electrolyte with Zn anode, while 1 m ZSO-H_2O electrolyte and 1 m ZOT-H_2O electrolyte were selected as comparisons. Figure 2(a) displays the voltage-time profiles of Zn/Zn symmetric cells at a current density of 1.0 mA cm^{-2} with a capacity of 1.0 mAh cm^{-2} each cycle. The cell with 1 m ZOT-H_2O-60% PEG electrolyte exhibits a high cycling stability over 3000 h without any evident voltage hysteresis or overpotential increase, in contrast to those in aqueous electrolytes with short lifespan and apparent voltage fluctuation. The corresponding enlarged discharge/charge curves are provided in Figure S8. The outstanding Zn plating/stripping stability over 2000 h at the current densities of 0.1, 0.25 and 0.5 mA cm^{-2} are also shown in Figure S9. Besides, the polarization voltages increase

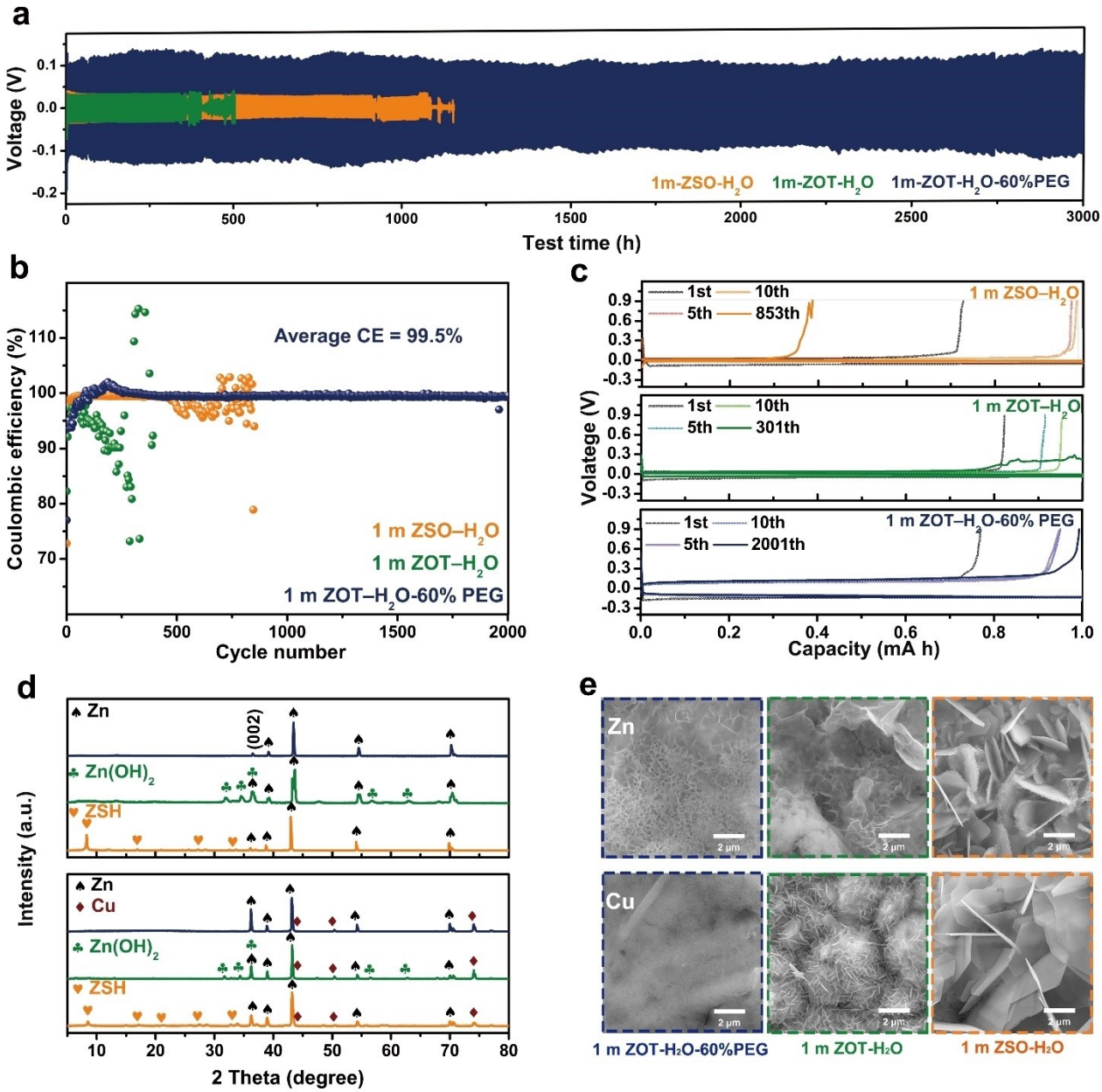

Figure 2. Zn^{2+} plating/stripping behaviors in 1 m ZSO-H_2O (orange), 1 m ZOT-H_2O (green) and 1 m ZOT-H_2O-60% PEG (blue) electrolytes. a) Comparison of voltage profiles of three electrolytes at 1 mA cm^{-2} and with a capacity of 1 mAh cm^{-2}. b) Zn plating/stripping CE values of Zn/Cu cells in different electrolytes. c) Typical voltage profiles of Zn/Cu cells at 1 mA cm^{-2}. d) XRD patterns in different elelctrolyte, the above range is Zn electrodes after stripping of 10 mAh, the below range is Cu electrodes after Zn plating of 10 mAh. e) SEM microscopy studies of Zn electrodes (the above range) and Cu electrodes (the below range) after plating of 10 mAh in different electrolytes.

as the ratio of PEG increases due to the coordination environment and the viscosity change in the hybrid electrolyte system (Figure S10).

The Coulombic efficiency (CE) of Zn plating/stripping in Zn/Cu asymmetric cells was recorded at a current density of 1.0 mA cm^{-2}, a deposition capacity of 1.0 mAh and a cut-off voltage of 0.9 V vs. Zn^{2+}/Zn, as shown in Figure 2(b). Clearly, the reversibility and stability of Zn anode in 1 m ZOT-H_2O-60% PEG electrolyte is significantly improved in comparison to that of aqueous electrolytes. Impressively, an average CE of 99.5% is maintained after 2000 cycles for hybrid electrolyte. In contrast, the CEs of cell with 1 M ZSO-H_2O and 1 m ZOT-H_2O shows a dreadful Zn plating/stripping process after 500 and 200 cycles, respectively. The lower CE with unstable stripping process in aqueous electrolytes could attribute to the side reactions between H_2O and Zn anode.[36] Although the typical Zn plating/striping profiles of Zn/Cu cell with hybrid electrolyte exhibits a slight increase of the overpotential (separation of charge/discharge potential) initially, it can stabilize at ~350 mV after 100 cycles and even up to 2000 cycles (Figure 2c).

In order to understand the significant difference of Zn depositing behavior between hybrid electrolyte and conventional aqueous electrolytes, Zn/Cu cells are investigated by depositing a certain amount capacity of 10 mAh.[29] After deposition, the XRD patterns of Zn anode in 1 M ZOT-H_2O-60% PEG electrolyte shows no byproducts (Figure 2d), while in aqueous electrolytes emerge several new peaks corresponding to byproducts, such as $Zn(OH)_2$/ZnO and $Zn_4SO_4(OH)_6 \cdot xH_2O$ (ZSH). It demonstrates that the introduction of PEG can significantly inhibit the side reactions at the interfaces. Concomitantly, Zn has a weaker (002) intensity in aqueous electrolytes than that in the hybrid electrolyte. The introduction of PEG changes the Zn deposition orientation in which (002) facets occupy a higher percentage, dendrite formation is less likely.[37] Scanning electron microscopy (SEM) images after discharging in 1 m ZOT-H_2O-60% PEG shows a highly porous inter-connected surface of Zn anode and a smooth flat of Cu electrode, as shown in Figure 2(e). While Zn deposition on the surface of Cu electrode in 1 m ZOT-H_2O are uneven distribution of spherical deposition with small flakes covered.[38,39] From the SEM images at low magnification (Figure S11e and f), the deposited Zn on Cu electrodes in aqueous electrolytes shows lots of protrusions. For 1 m ZSO-H_2O, both Zn and Cu electrodes surfaces are covered by lots of hexagonal lamellar shapes corresponding to ZSH, which is confirmed by literatures.[40] Such side reactions (dendrite, water splitting and corrosion) in aqueous electrolytes would be detrimental for large-scale practical application of ZIBs.[41] These results grades water-PEG a much superior hybrid solvent over water for a lowered possibility of side reactions and the dendrite-free Zn plating/stripping.

Effect of hybrid electrolyte on the stability of full batteries

The effect of as-prepared hybrid electrolyte on the stability of full batteries was further revealed in this section, based on HVO cathode, which was characterized in detail in Figure S12. As expected, hybrid electrolyte shows a huge preponderance with the match of HVO (Figure S13), and a stable capacity retention can be achieved when PEG content is above 50%. For instance, the Zn/HVO cell with 1 m ZOT-H_2O-60% PEG electrolyte delivered a high capacity of 372.3 mAh g^{-1} with the reversible charge-discharge curves at 0.1 A g^{-1} and maintained the best capacity retention of 96% after 50 cycles (Figure S14), while cells with aqueous electrolyte displayed a serious performance deterioration. Besides, Zn/HVO cells with different electrolytes at the current density of 1 A g^{-1} were tested (Figure S15). For aqueous electrolytes, the initial capacity of 345 mAh g^{-1} was achieved, but followed a serious capacity attenuation. By contrast, Zn/HVO cell with 1 m ZOT-H_2O-60% PEG electrolyte exhibited good cycling stability.

In order to simulate the stability under actual application environment with the characteristics of intermittent use, a reliable test mode containing the cycling capacity and the anti-self-discharge behavior is needed to evaluate the reliability of Zn/HVO batteries.[42] In details, the batteries are fully discharged/charged for 8 cycles and then leave for 24 h at the open circuit, which has been recycled up to 50 cycles. As shown in Figure 3a–c, the capacity of batteries with aqueous electrolytes decreases dramatically after shelving, while it is maintained well in the hybrid electrolyte. After the first shelving for 24 h, a higher CE of 97.1% was achieved in hybrid electrolyte, which is much higher than that in aqueous electrolytes (inset in Figure 3c). The recoverable capacity retention after 24-hour rest in aqueous electrolytes is around 80% with a slight upward trend (Figure S16). Significantly, the voltage-time curve of the battery with hybrid electrolyte shows a steep drop corresponding with overpotential at first and a subsequent flat trend during shelving. However, the batteries with aqueous electrolytes show a slanting downward trend corresponding to the self-discharging process.[31] A comparison of the cycling performance at the same time between the common cycle test and rest-cycle test shows that the duration time seems to be the key factor for capacity attenuation (Figure S17). The capacity attenuation during shelving in aqueous electrolyte could be ascribed to the dissolution of cathode and self-discharging.[43]

Figure 3(d) shows the solubility of HVO cathode in electrolytes for different soaking time at room temperature. The 1 m ZOT-H_2O-60% PEG electrolyte remains colorless and transparent after 50 days of electrode immersion, whereas the aqueous electrolytes turn to light yellow after 2 days. Generally, V_2O_5 is slightly soluble in aqueous solution,[44] which caused by the water molecules. Vanadium dissolution is ubiquitous in aqueous electrolyte due to the inferior structural stability and the chemical dissolution with the formation of soluble V-based specie, which leads to structural degradation.[45] The amount of active water on the cathode/electrolyte interface and the dissolubility would be two determining factors for V dissolution. The inductive coupled plasma emission spectrometry (ICP) results reveal that the dissolution of V element could be effectively alleviated in hybrid electrolyte (Figure 3e). Importantly, the Zn^{2+} ions content in aqueous electrolytes is lower

Research Article
doi.org/10.1002/batt.202200001
Chemistry Europe
European Chemical Societies Publishing

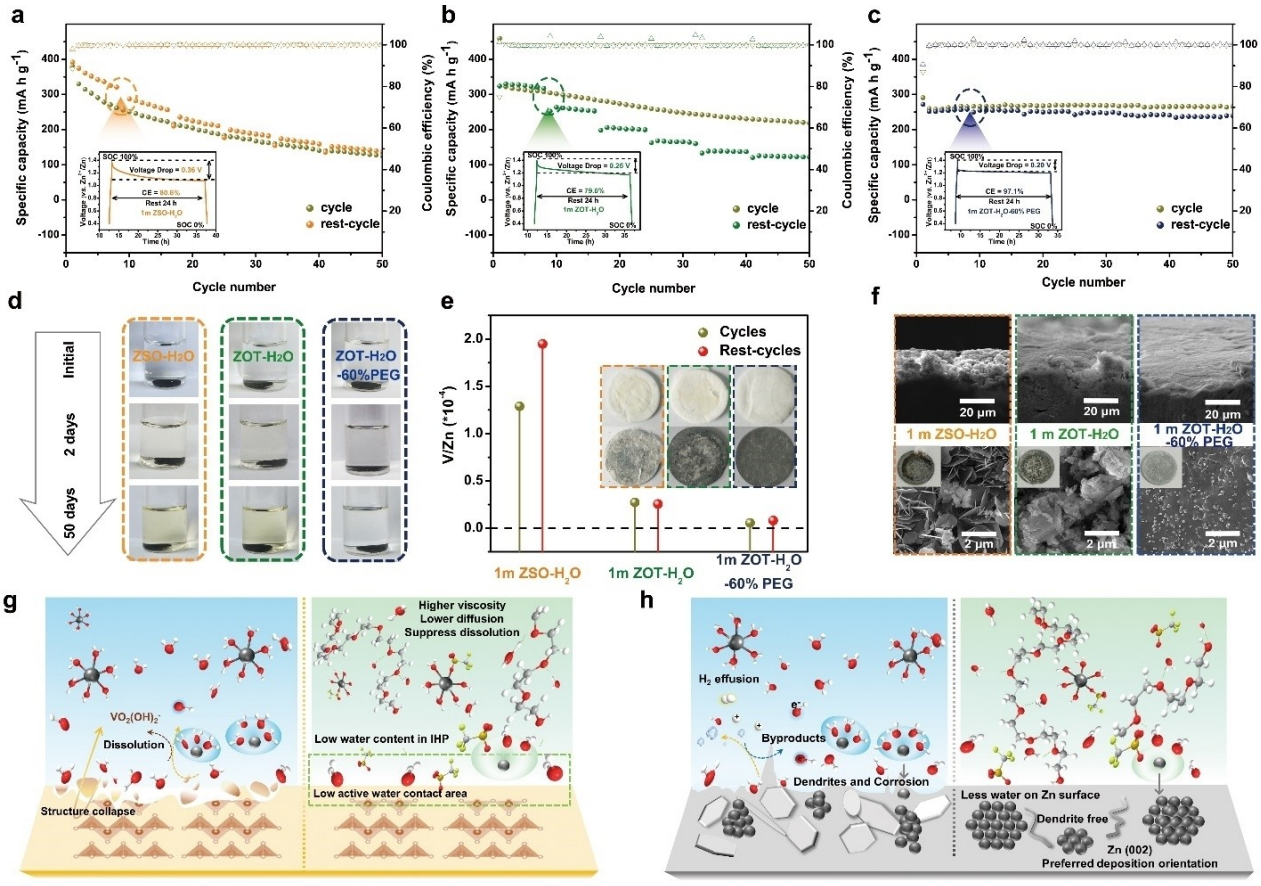

Figure 3. Storage performance comparison of Zn/HVO batteries evaluated by resting for 24 h at 100% state of charge (SOC) after per 8 cycles at 0.5 A g^{-1}, followed by full discharging: a) 1 m ZSO-H_2O, b) 1 m ZOT-H_2O, c) 1 m ZOT-H_2O-60% PEG. Insets show the charge-discharge curves during resting for 24 h at fully charged state after the first 8 cycles at 0.5 A g^{-1}. d) Optical images of HVO electrodes immersed in different electrolytes for different periods. e) ICP results of Zn and V in the Zn/HVO after 8 cycles and 8 cycles-24 h rest. Insets are pictures of the corresponding membrane and anode. f) SEM images of Zn electrode in Zn/HVO batteries with different electrolytes. The top row of images are the lateral surfaces of Zn anode; the below one are the anode surfaces. Insets show the optical images of cycled Zn electrodes. Schematic illustration of interfacial reactions in aqueous and hybrid electrolytes: g) cathode/electrolyte interface, h) anode/electrolyte interface.

than that in 1 m ZOT-H_2O-60% PEG electrolyte, which could attribute to the irreversible consumption of electrolyte (Tables S2 and S3). As shown in Figure S18, there is a lot of deciduous material on the membranes on cathode side in the Zn/HVO aqueous cells after cycles. Beyond that, more severe apparent condition (many black pits) on the separator surface of the anode side is observed. According to the XRD results (Figure S19), by-products (ZSH, $Zn_x(CF_3SO_3)_y(OH)_{2x-y}\cdot nH_2O$ (denote as ZFH) and ZnO) are directly observed in 1 m ZSO-H_2O and 1 m ZOT-H_2O, respectively. And the peak intensity of by-products increased for the samples after 5 times of 24-hour rest during cycling. The formation of basic zinc slats might follow similar process proposed by previous works in aqueous electrolytes, which derived from the decomposition of water and the formation of OH^-. This finding suggests the side reactions on anode interface were still going on during shelving time in aqueous electrolyte.

As for 1 m ZOT-H_2O-60% PEG electrolyte, there is no peaks corresponding to byproducts, indicating the excellent electrochemical stability of electrolyte. Here the introduction of PEG suppresses the activities of water. Additionally, unlike the pristine XRD pattern for metallic Zn and that after cycling in aqueous electrolytes, the peak intensity of Zn (002) electrode changes significantly in 1 m ZOT-H_2O-60% PEG, which is consistent with the XRD data in asymmetric batteries. From the SEM images (Figures 3f and S20), it was observed that the Zn anode surface is covered many aggregated schistose by-products in aqueous electrolyte. The uneven anode surface shows more cracks and protrusions clustered together in aqueous electrolyte after 24*5 hours rest-cycles process.

According to the above discussion, the effects of hybrid electrolyte on the stability of full batteries are reflected at both cathode side and anode side. The addition of PEG greatly reduced the active water in the inner Helmholtz plane (IHP), thus, reducing the chances for cathode contact to lots of active water (Figure 3g).[46] According to the Stokes-Einstein equation, the diffusion coefficient is inversely proportional to the viscosity.[47] The addition of PEG alleviates the dissolution of cathode. The longer duration time under low current densities provide plenty of time for cathode dissolution and the diffusion of V species leached out from cathode. As a consequence, the closely interconnected parasitic reactions combine to lead to

Research Article
doi.org/10.1002/batt.202200001
Chemistry Europe
European Chemical Societies Publishing

the interfacial degradation of Zn/HVO batteries. By comparison, a uniform Zn deposition surface is observed even after 24× 5 hours rest-cycle process for the Zn/HVO batteries with 1 m ZOT-H_2O-60% PEG electrolyte. The hydrogen evolution and formation of by-products are easily occurred on the anode interface in aqueous electrolyte. By contrast, the zinc deposition is smooth in hybrid electrolyte. The addition of long-chain-structure PEG restricts the lateral 2D diffusion of Zn^{2+} ions from solution and prevents the growth of large dendrites, which can slow down the nucleation and growth of zinc deposits.[48] On account of the limitation of PEG to active water and the strong absorption of PEG on zinc anode, the sediments show a smoothing surface (Figure 3h).

Electrochemical performance and practical verification of batteries with hybrid electrolyte

As revealed above, the hybrid electrolyte contributes good cycling stability to V-based materials at low current densities. Besides, HVO cathode displays an excellent capability at high rates (above 2 A g^{-1}) in aqueous electrolytes (Figure S21). While the capacity retention ratio of the cell with 1 m ZOT-H_2O electrolyte down from 44% to 10% at 5 A g^{-1} after rate-rest test (Figure 4a). The rate capability of coin cell with 1 m ZOT-H_2O-60% PEG electrolyte was further investigated as shown in Figure S22(a), in which an average capacity recovers to 342 mAh g^{-1} as the rate resumes to 0.1 A g^{-1}. The Zn/HVO batteries with 1 m ZOT-H_2O-60% PEG electrolyte displayed a super stable capability, in which a capacity retention of 82.4% at 0.5 A g^{-1} after 500 cycles was achieved even after the first 120-hour shelving time (Figrue S22b). Moreover, a long-life span after 1000 cycles with a capacity retention of 71.4% at 0.5 A g^{-1} was achieved (Figure 4b), indicating the super stable performance. In contrast, Zn/HVO cells with 1 m ZOT-H_2O electrolyte failed within 120 cycles at the same test condition (Figure S22c). These results indicate that the performance of Zn/HVO batteries with hybrid electrolyte were greatly improved. Impressively, the cell with 1 m ZOT-H_2O-90% PEG exhibited significantly boosted cycling stability, together with a capacity retention of 80% after 1000 cycles at 100 mA g^{-1} but with a low capacity of ~140 mAh g^{-1}, which took up over 3200 h (Figure S22d).

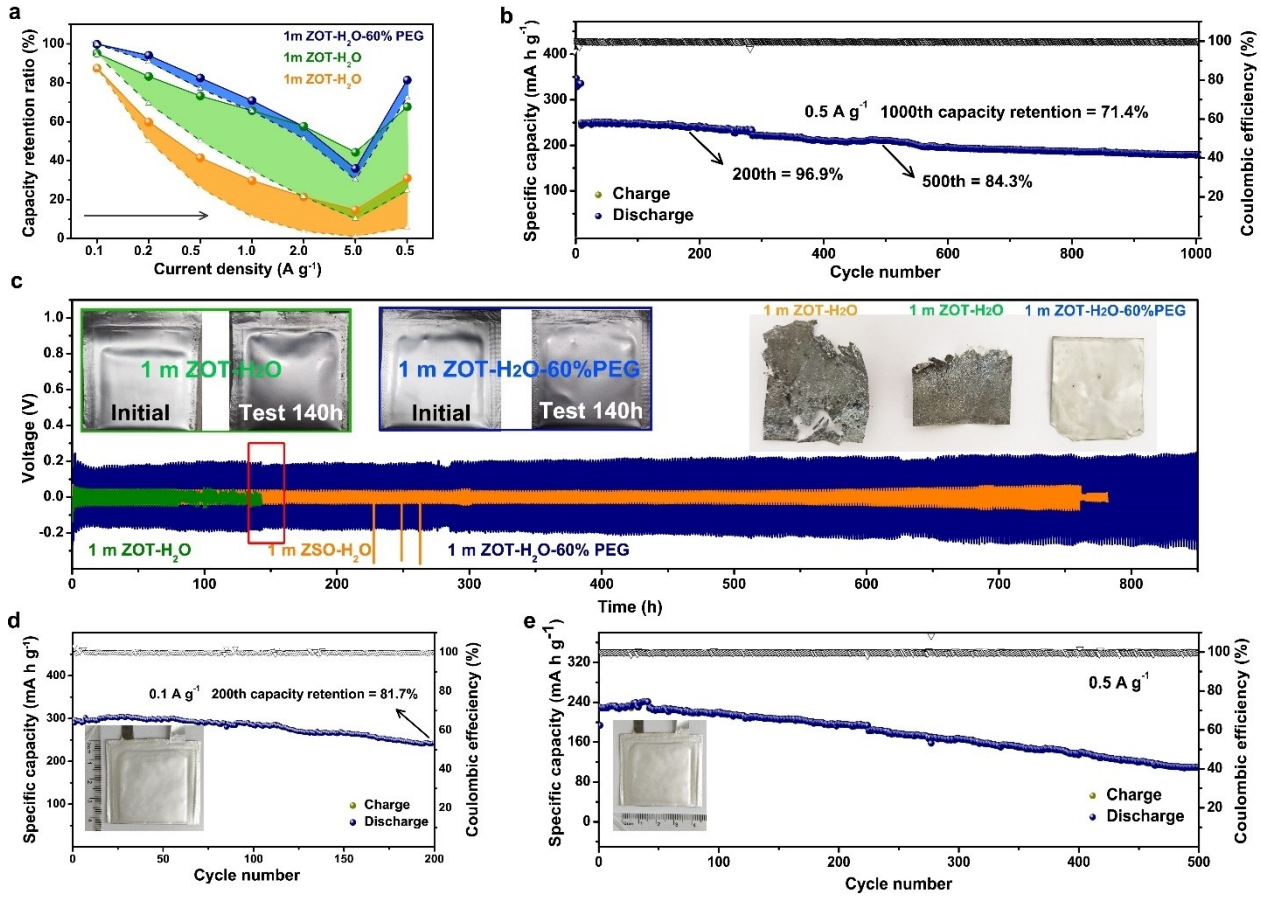

Figure 4. a) Capacity retention ratio for common rate (solid line) and rest-rate (dotted line) test of Zn/HVO coin cells with 1 m ZOT-H_2O-60% PEG (blue), 1 m ZOT-H_2O (green) and 1 m ZSO-H_2O (orange) electrolytes. b) Long cycling performances of Zn/HVO coin cells at 0.5 A g^{-1}. c) Zn symmetric pouch cell (3 cm × 3 cm) with a capacity of 1 mAh cm^{-2} under a current density of 1 mA cm^{-2}. The insets are optical images of pouch cell before/after cycles and zinc anodes after long-term cycling and soaking time under room temperature (in total: 60 days). The cyclic performance of Zn/HVO pouch cells at a current density of d) 0.1 A g^{-1} and e) 0.5 A g^{-1}.

In order to verify the practicability of this system, we further evaluate it in pouch cells.[49] The pouch Zn/Zn symmetric cell with 1 m ZOT-H_2O-60 % PEG electrolyte exhibits a higher cyclic stability over 850 h than that in 1 m ZOT-H_2O electrolyte and 1 m ZSO-H_2O electrolyte (Figure 4c). The insets in Figure 4(c) show that Zn/Zn pouch cell with hybrid electrolyte does not exhibit inflated, while a significant bulge can be seen in 1 m ZOT-H_2O electrolyte after only 140 h, leading to a degradation of Zn^{2+} plating/striping. What's more, the optical pictures of zinc anodes after long-term cycling display that zinc metal in aqueous electrolyte is severely corroded, showing a fragmentary appearance of fragility. In comparison, zinc anode maintains good integrity and flexibility in hybrid electrolyte. Although pure aqueous electrolytes are inherently safe, the triggered fatal issues such as gas production and pulverization of zinc anode make them difficult to match in practical applications.

The Zn/HVO pouch cells with the size of 3 cm in length and 3 cm in width were further assembled to evaluate the practicability of hybrid electrolyte. The pouch cell with an active mass load of 11.7 mg, exhibited good cycling stability with a high capacity of 300 mAh g^{-1} and 81.7 % retention after 200 cycles under a current density of 0.1 A g^{-1}, as shown in Figure 4(d). Even with a high mass load of 20.79 mg, the pouch cell also displayed a high capacity of 203 mAh g^{-1} after 200 cycles (Figure S23). More importantly, the pouch cell showed good cycling performance with a capacity of 109.9 mAh g^{-1} after 500 cycles under a current density of 0.5 A g^{-1}. Zn/HVO pouch cells exhibits superior capacity retention than that of other Zn/vanadium pouch cells in previous reports, such as Zn/$NaV_3O_8 \cdot 1.5H_2O$ batteries with gelation electrolyte,[50] Zn/La-V_2O_5 batteries with 1 m ZOT aqueous electrolyte[51] and Zn/vanadium oxides with 4 m ZOT aqueous electrolyte[52] and so on (Table S4).

Conclusion

In summary, hybrid electrolyte by introducing PEG 400 as co-solvent was developed for stable ZMBs with HVO cathode in this work. The hybrid electrolyte containing high proportion of PEG 400 to enable ZMBs with high reversibility, long stability and safety. PEG 400 with lots of nucleophilic groups can trammel the free water in the electrolyte, alleviating the water-induced reactions and exhibiting a wide ESW of 2.6 V. A good reversible zinc plating/stripping over 3000 h for Zn/Zn cell and an average CE of 99.5 % maintained over 2000 cycles for Zn/Cu cell were obtained, respectively. Zn/HVO cells with hybrid electrolyte exhibited excellent cycling stability without capacity fading after 50 cycles at low current density of 0.1 A g^{-1}. Particularly, the pouch cells of 3 cm × 3 cm exhibit a high capacity of 300 mAh g^{-1} at 0.1 A g^{-1} with a good retention of 81.7 % retention after 200 cycles, and even up to 500 cycles at 0.5 A g^{-1}, indicating a good practical prospect of this system.

Acknowledgements

This work was supported by the National Natural Science Foundation of China (Grant no. 52072411, 51932011), Natural Science Foundation of Hunan Province (Grant no. 2021JJ20060) and the Science and Technology Innovation Program of Hunan Province (Grant no. 2021RC3001).

Conflict of Interest

The authors declare no conflict of interest.

Data Availability Statement

Research data are not shared.

Keywords: hybrid electrolyte · polyethylene glycol · stability · vanadium-based materials · zinc-metal batteries

[1] L. E. Blanc, D. Kundu, L. F. Nazar, *Joule* **2020**, *4*, 771.
[2] D. Chao, W. Zhou, F. Xie, C. Ye, H. Li, M. Jaroniec, S. Z. Qiao, *Sci. Adv.* **2020**, *6*, eaba4098.
[3] Y. Liu, G. He, H. Jiang, I. P. Parkin, P. R. Shearing, D. J. L. Brett, *Adv. Funct. Mater.* **2021**, *31*, 2010445.
[4] Y. Liu, X. Lu, F. Lai, T. Liu, P. R. Shearing, I. P. Parkin, G. He, D. J. L. Brett, *Joule* **2021**, *5*, 2845.
[5] L. Kang, M. Cui, Z. Zhang, F. Jiang, *Batteries & Supercaps* **2020**, *3*, 966.
[6] G. Fang, J. Zhou, A. Pan, S. Liang, *ACS Energy Lett.* **2018**, *3*, 2480.
[7] Y. Liu, Y. Liu, Y. Yamauchi, Z. A. Alothman, Y. V. Kaneti, X. Wu, *Batteries & Supercaps* **2021**, *4*, 1867.
[8] J. Ding, Z. Du, L. Gu, B. Li, L. Wang, S. Wang, Y. Gong, S. Yang, *Adv. Mater.* **2018**, *30*, e1800762.
[9] M. Yan, P. He, Y. Chen, S. Wang, Q. Wei, K. Zhao, X. Xu, Q. An, Y. Shuang, Y. Shao, K. T. Mueller, L. Mai, J. Liu, J. Yang, *Adv. Mater.* **2018**, *30*, 1703725.
[10] Q. Zhang, K. Xia, Y. Ma, Y. Lu, L. Li, J. Liang, S. Chou, J. Chen, *ACS Energy Lett.* **2021**, *6*, 2704.
[11] N. Zhang, M. Jia, Y. Dong, Y. Y. Wang, J. Z. Xu, Y. C. Liu, L. F. Jiao, F. Y. Cheng, *Adv. Funct. Mater.* **2019**, *29*, 9.
[12] P. He, G. Zhang, X. Liao, M. Yan, X. Xu, Q. An, J. Liu, L. Mai, *Adv. Energy Mater.* **2018**, *8*, 1702463.
[13] D. Kundu, B. D. Adams, V. Duffort, S. H. Vajargah, L. F. Nazar, *Nat. Energy* **2016**, *1*, 1.
[14] Y. Zhang, F. Wan, S. Huang, S. Wang, Z. Niu, J. Chen, *Nat. Commun.* **2020**, *11*, 2199.
[15] X. Jia, C. Liu, Z. G. Neale, J. Yang, G. Cao, *Chem. Rev.* **2020**, *120*, 7795.
[16] M. Zhou, S. Guo, G. Fang, H. Sun, X. Cao, J. Zhou, A. Pan, S. Liang, *J. Energy Chem.* **2021**, *55*, 549.
[17] J. Cao, D. Zhang, R. Chanajaree, Y. Yue, Z. Zeng, X. Zhang, J. Qin, *Adv. Powder Mater.* **2021**, *10*.1016/j.apmate.2021.09.007.
[18] K. Xu, *Chem. Rev.* **2014**, *114*, 11503.
[19] Z. Liu, X. Luo, L. Qin, G. Fang, S. Liang, *Adv. Powder Mater.* **2021**, *10*.1016/j.apmate.2021.10.002.
[20] M. Winter, B. Barnett, K. Xu, *Chem. Rev.* **2018**, *118*, 11433.
[21] S. B. Wang, Q. Ran, R. Q. Yao, H. Shi, Z. Wen, M. Zhao, X. Y. Lang, Q. Jiang, *Nat. Commun.* **2020**, *11*, 1634.
[22] T. Zhang, Y. Tang, S. Guo, X. Cao, A. Pan, G. Fang, J. Zhou, S. Liang, *Energy Environ. Sci.* **2020**, *13*, 4625.
[23] L. Zhang, I. A. Rodríguez-Pérez, H. Jiang, C. Zhang, D. P. Leonard, Q. Guo, W. Wang, S. Han, L. Wang, X. Ji, *Adv. Funct. Mater.* **2019**, *29*, 1902653.
[24] L. M. Suo, O. Borodin, T. Gao, M. Olguin, J. Ho, X. L. Fan, C. Luo, C. S. Wang, K. Xu, *Science* **2015**, *350*, 938.
[25] Y. Yamada, J. Wang, S. Ko, E. Watanabe, A. Yamada, *Nat. Energy* **2019**, *4*, 269.

[26] J. Hao, L. Yuan, C. Ye, D. Chao, K. Davey, Z. Guo, S. Z. Qiao, *Angew. Chem. Int. Ed. Engl.* **2021**, *60*, 7366.
[27] R. Qin, Y. Wang, M. Zhang, Y. Wang, S. Ding, A. Song, H. Yi, L. Yang, Y. Song, Y. Cui, J. Liu, Z. Wang, S. Li, Q. Zhao, F. Pan, *Nano Energy* **2021**, *80*, 105478.
[28] J. Chen, J. Vatamanu, L. Xing, O. Borodin, H. Chen, X. Guan, X. Liu, K. Xu, W. Li, *Adv. Energy Mater.* **2019**, *10*, 1902654.
[29] L. Cao, D. Li, E. Hu, J. Xu, T. Deng, L. Ma, Y. Wang, X. Q. Yang, C. Wang, *J. Am. Chem. Soc.* **2020**, *142*, 21404.
[30] Q. Nian, J. Wang, S. Liu, T. Sun, S. Zheng, Y. Zhang, Z. Tao, J. Chen, *Angew. Chem. Int. Ed. Engl.* **2019**, *58*, 16994.
[31] Y. Dong, L. Miao, G. Ma, S. Di, Y. Wang, L. Wang, J. Xu, N. Zhang, *Chem. Sci.* **2021**, *12*, 5843.
[32] J. Xie, Z. Liang, Y. C. Lu, *Nat. Mater.* **2020**, *19*, 1006.
[33] H. E. Gottlieb, V. Kotlyar, A. Nudelman, *J. Org. Chem.* **1997**, *62*, 7512.
[34] V. D. Noto, M. Vittadello, G. Pace, S. Biscazzo, S. Lavina, *Macromol. Chem. Phys.* **2002**, *203*, 1201.
[35] J. Pavelec, D. DiGuiseppi, B. Y. Zavlavsky, V. N. Uversky, R. Schweitzer-Stenner, *J. Mol. Liq.* **2019**, *275*, 463.
[36] C. Li, X. Xie, S. Liang, J. Zhou, *Energy Environ. Mater.* **2020**, *3*, 146.
[37] M. Zhou, S. Guo, J. Li, X. Luo, Z. Liu, T. Zhang, X. Cao, M. Long, B. Lu, A. Pan, G. Fang, J. Zhou, S. Liang, *Adv. Mater.* **2021**, *33*, e2100187.
[38] F. Wang, O. Borodin, T. Gao, X. Fan, W. Sun, F. Han, A. Faraone, J. A. Dura, K. Xu, C. Wang, *Nat. Mater.* **2018**, *17*, 543.
[39] C. Zhang, J. Holoubek, X. Wu, A. Daniyar, L. Zhu, C. Chen, D. P. Leonard, I. A. Rodriguez-Perez, J. X. Jiang, C. Fang, X. Ji, *Chem. Commun. (Camb.)* **2018**, 54, 14097.
[40] T. Zhang, Y. Tang, G. Fang, C. Zhang, H. Zhang, X. Guo, X. Cao, J. Zhou, A. Pan, S. Liang, *Adv. Funct. Mater.* **2020**, *30*, 2002711.
[41] L. Ma, M. A. Schroeder, T. P. Pollard, O. Borodin, M. S. Ding, R. Sun, L. Cao, J. Ho, D. R. Baker, C. Wang, K. Xu, *Energy Environ. Mater.* **2020**, *3*, 516.
[42] L. Zhang, B. Zhang, J. Hu, J. Liu, L. Miao, J. Jiang, *Small Methods* **2021**, *5*, 2100094.
[43] F. Zhang, X. Sun, M. Du, X. Zhang, W. Dong, Y. Sang, J. Wang, Y. Li, H. Liu, S. Wang, *Energy Environ. Mater.* **2020**, *0*, 1.
[44] Y. Lu, T. Zhu, W. van den Bergh, M. Stefik, K. Huang, *Angew. Chem. Int. Ed. Engl.* **2020**, *59*, 17004.
[45] G. Yang, Q. Li, K. Ma, C. Hong, C. Wang, *J. Mater. Chem. A* **2020**, *8*, 8084.
[46] J. Yue, L. Lin, L. Jiang, Q. Zhang, Y. Tong, L. Suo, Y. s. Hu, H. Li, X. Huang, L. Chen, *Adv. Energy Mater.* **2020**, *10*, 2000665.
[47] A. A. Noyes, W. R. Whitney, *J. Am. Chem. Soc.* **1897**, *19*, 930.
[48] A. Mitha, A. Z. Yazdi, M. Ahmed, P. Chen, *ChemElectroChem* **2018**, *5*, 2409–2418.
[49] Y. Li, Z. Wang, Y. Cai, M. E. Pam, Y. Yang, D. Zhang, Y. Wang, S. Huang, *Energy Environ. Mater.* **2021**, *10*.1002/eem2.12265.
[50] F. Wan, L. Zhang, X. Dai, X. Wang, Z. Niu, J. Chen, *Nat. Commun.* **2018**, *9*, 1656.
[51] D. Zhang, J. Cao, Y. Yue, T. Pakornchote, T. Bovornratanaraks, J. Han, X. Zhang, J. Qin, Y. Huang, *ACS Appl. Mater. Interfaces* **2021**, *13*, 38416.
[52] F. Wan, Z. Hao, S. Wang, Y. Ni, J. Zhu, Z. Tie, S. Bi, Z. Niu, J. Chen, *Adv. Mater.* **2021**, *33*, 2102701.

Manuscript received: January 3, 2022
Revised manuscript received: January 24, 2022
Version of record online: February 22, 2022